1,2-Hydroxypyridonates as Contrast Agents for Magnetic Resonance Imaging: TREN-1,2-HOPO[1]

*Christoph J. Jocher,[†] Evan G. Moore,[†] Jide Xu,[†] Stefano Avedano, [‡] Mauro Botta,[‡] Silvio Aime,[§] and Kenneth N. Raymond[†]**

Department of Chemistry, University of California, Berkeley, CA 94720-1460, Dipartimento di Scienze dell´Ambiente e della Vita, Università del Piemonte Orientale "A. Avogadro", Via Bellini 25/G, I-15100 Alessandria, Italy, and Dipartimento di Chimica I. F. M., Università di Torino, Via P. Giuria 7, I-10125 Torino, Italy.

AUTHOR EMAIL ADDRESS raymond@socrates.berkeley.edu

RECEIVED DATE (to be automatically inserted after your manuscript is accepted if required according to the journal that you are submitting your paper to)

TITLE RUNNING HEAD. [Gd(TREN-1,2-HOPO)(H_2O)$_2$] for MRI

CORRESPONDING AUTHOR FOOTNOTE.

Telephone number +1 (510) 642 7219, fax numbers +1 (510) 486-5283.

ABSTRACT. 1,2-Hydroxypyridinones (1,2-HOPO) form very stable lanthanide complexes that may be useful as contrast agents for Magnetic Resonance Imaging (MRI). X-ray diffraction of single crystals established that the solid state structures of the Eu(III) and the previously reported [*Inorg. Chem.* **2004**, *43*, 5452] Gd(III) complex are identical. The recently discovered sensitizing properties of 1,2-HOPO chelates for Eu(III) luminescence allow direct measurement of the number if water molecules in the

metal complex. Fluorescence measurements of the Eu(III) complex corroborate that in solution two water molecules coordinate the lanthanide (q = 2) as proposed from the analysis of NMRD profiles. In addition, fluorescence measurements have verified the anion binding interactions of lanthanide TREN-1,2-HOPO complexes in solution, studied by relaxivity, revealing only very weak oxalate binding (K_A = 82.7 ± 6.5 M^{-1}). Solution thermodynamic studies of the metal complex and free ligand have been carried out using potentiometry, spectrophotometry and fluorescence spectroscopy. The metal ion selectivity of TREN-1,2-HOPO supports the feasibility of using 1,2-HOPO ligands for selective lanthanide binding [pGd = 19.3 (2); pZn = 15.2 (2), pCa = 8.8 (3)].

KEYWORDS. 1,2-Hydroxypyridonate, Gadolinium, Europium, MRI, Fluorescence, Chelate stability, Selectivity, Solution thermodynamics.

Introduction

High chelate stability is essential for lanthanide complexes in medicine because lanthanide ions have known toxicity via their interaction with Ca(II) binding sites.[2] Additionally, the application of weak Gd(III) chelators as MRI contrast agent (MRI-CA) can cause nephrogenic systemic fibrosis in patients with low kidney activity.[3] To date gadolinium based contrast agents for magnetic resonance imaging (MRI-CA) used clinically rely on conveniently available aminocarboxylate chelates derived from DTPA and macrocyclic DOTA.[4] However, the weak Gd(III) nitrogen bond does not significantly contribute to chelate stability in these compounds. Thus, only octadentate ligands provide sufficient chelate stability, which limits the number of coordinated water molecules to one (q = 1). The resulting limit in relaxivity can be circumvented by utilizing the known oxophilicity of lanthanides. Purely oxygen donor ligands such as hydroxypyridinone (HOPO, Chart 1) and terephthalamide (TAM) chelates allow two[5] or three[6] coordinated water molecules (q = 2 or 3) at the metal center without destroying chelate stability, and have been established as candidates for high relaxivity next generation contrast agents. These ligands combine enhanced relaxivity and high stability – a combination

considered impossible for small molecular weight MRI-CA based on aminocarboxylate ligands.[7] The further development of mixed 3,2-HOPO-TAM chelates follows the current trend of improving relaxometric properties of MRI-CA by formation of polymers[8], dendrimers[9] or supramolecular compounds.[10] The feasibility of applying such 3,2-HOPO chelates as MRI-CA has been proven successfully *in vivo*.[11]

It has been one of the very few disfavored features of 3,2-HOPO that the solution structure of its lanthanide complexes cannot be elucidated by other means than relaxometry. Methods such as Dy(III) induced paramagnetic shift in ^{17}O-NMR spectroscopy,[12] or fluorescence spectroscopy of parent Eu(III) or Tb(III) chelates[13] have been investigated without much success. As such, information about the solution structure including the hydration number *q* for 3,2-HOPO and TAM chelates has been inferred only by relaxometry based on reasonable assumptions about the values of several parameters and, whenever possible, on the comparison of ^{1}H and ^{17}O NMR relaxation data. The recent discovery of the excellent luminescence sensitizing properties of 6-carboxylamide-1,2-hydroxypyridonates (1,2-HOPO) for Eu(III)[14] allows the correlation of relaxometric data with fluorescence spectroscopy for 1,2-HOPO compounds. Contrary to several well studied 3,2-HOPO chelates, only TREN-1,2-HOPO[15] and TACN-1,2-HOPO[6] have been described as 1,2-HOPO chelates for MRI contrast agents. Comparison of the solid state structure and NMRD profile of Gd-TREN-1,2-HOPO with Gd-TREN-3,2-HOPO led to the conclusion that these complexes behave very similarly in solution.[15]

Thus, 1,2-HOPO can be used as a fluorescent tool to elucidate solution structure of HOPO chelates by fluorescence spectroscopy in addition to relaxometry and solution thermodynamics. The following contribution presents details on solution stability and structure of the Eu(III), Gd(III) and Zn(II) complexes of TREN-1,2-HOPO. For the first time, fluorescence spectroscopy of a TREN-HOPO chelate as the Eu(III) complex are used to support solution structure assignments based on relaxivity measurements for the same ligand with Gd(III). This comparative study of relaxometric data of the

Gd(III)-TREN-1,2-HOPO complex and luminescence data of the isostructural Eu(III) complex was also applied for determining binding affinities of bioavailable and synthetically interesting anions for the Eu(III) and Gd(III) complexes of TREN-1,2-HOPO and to assign the structure of ternary complexes in solution. In addition, solution thermodynamic stability was assessed for an estimate of potential toxicity of TREN-1,2-HOPO chelates.

Experimental details

General

All chemicals were used as received from Aldrich unless otherwise noted. TREN-1,2-HOPO[15] and 3-benzoxy-4-carboxy-2-pyridone (3,2-HOPO(Bn) acid)[5] were synthesized as previously reported. ^{1}H and ^{13}C NMR spectra were obtained on Bruker AVQ-400 spectrometers and are reported in ppm. Mass spectra and elemental (CHN) analyses were performed at the Elemental Analysis Facility, College of Chemistry, UC Berkeley. Unless specified, solvents were removed by rotary evaporation.

Synthesis

3-Benzyloxy-4-methylcarbamido-1-methyl-2-pyridone

3-Benzyloxy-4-carboxy-1-methyl-2-pyridone (2.56 g, 10 mmol) was dissolved in toluene (10 mL). Oxalylchloride (3.81 g, 30 mmol) and three drops of DMF were added. Volatiles were removed after gas evolution ceased (~ 1 hr) and the remaining solid was dissolved in dry THF (50 mL). Methylamine (40 % in water; 50 mL) was diluted with THF (50 mL), cooled on an ice bath and the solution of 3-benzyloxy-4-carboxychloro-1-methyl-2-pyridone was added. The reaction mixture was stirred on an ice bath for 4 hr. and dichloromethane (250 mL) was added. The reaction mixture was washed with 1 M HCl (3 x 100 mL), 1 M KOH (3 x 100 mL) and water (1 x 50 mL) and dried over Na_2SO_4. Volatiles were removed under reduced pressure and a yellowish solid remained. Yield: 2.34 g (8.59 mmol, 86 %) **^{1}H NMR** ($CDCl_3$, 400.132 MHz) δ = 7.89 (s, 1 H, amide NH), 7.43-7.33 (m, 5 H, Bn-CH), 7.13 (d, 1 H,

6-CH_{HOPO}, $^3J_{HH}$ = 7.2 Hz), 6.78 (d, 1 H, 6-CH_{HOPO}, $^3J_{HH}$ = 7.2 Hz), 5.54 (s, 2 H, OCH_2Ph), 3.59 (s, 3 H, $N_{HOPO}CH_3$), 2.78 (d, 3 H, . 4-CONHC*H*$_3$, $^2J_{HH\ vic}$= 5.2 Hz). **^{13}C NMR** ($CDCl_3$, 100.623 MHz) δ = 163.8 (CONH), 159.7 (CONH), 146.4, 136.2, 132.2, 130.8 (ipso-C-Bn), 129.1 (Ph-CH), 128.9 (Ph-CH), 128.8 (Ph-CH), 128.4, 126.9, 104.9 (5-CH_{HOPO}), 65.1 (OCH_2Ph), 37.7 (1-NCH_3), 26.3 (4-CONH*C*H_3). **ESI-MS** (MeOH) *m/z* = 567.2 (95 %, $[2M+Na]^+$), 295.2 (100 %, $[MNa]^+$).

3-Hydroxy-4-methylcarbamido-1-methyl-2-pyridone

3-Benzyloxy-4-methylcarbamido-1-methyl-2-pyridone (2.34 g, 8.59 mmol) was dissolved in acetic acid (6 mL). Hydrochloric acid (6 mL) was added and the solution was stirred for 18 hrs. Solvents were removed under reduced pressure. Water (100 mL) was added to the remaining yellowish suspension. The mixture was extracted with methylene chloride (2x 100 mL) and the remaining colorless suspension was filtered. Concentration of the filtrate allowed the collection of a second crop of the title compound as colorless needles. Combined yield: 658 mg (3.61 mmol, 42 %). Melting point: 201°C. fw = 182.18 g/mol. Anal. for $C_8H_{10}N_2O_3$ calcd. (found): C 52.74 (52.37), H 5.53 (5.59), 15.38 (14.99). **^{1}H NMR** (d_6-DMSO, 400.132 MHz) δ = 11.7 (s br, 1 H, OH), 8.40 (d, 1 H, amide NH), 7.15 (d, 1 H, 6-CH_{HOPO}, $^3J_{HH}$ = 7.2 Hz), 6.46 (d, 1 H, 6-CH_{HOPO}, $^3J_{HH}$ = 7.2 Hz), 3.43 (s, 3 H, $N_{HOPO}CH_3$), 2.77 (d, 3 H, . 4-CONHC*H*$_3$, $^2J_{HH\ vic}$= 5.2 Hz). **^{13}C NMR** (d_6-DMSO, 100.623 MHz) δ = 166.6 (CONH), 158.4 (CONH), 148.3, 128.1, 117.3, 102.7 (5-CH_{HOPO}), 37.2 (1-NCH_3), 26.5 (4-CONH*C*H_3). **FAB-MS** (NBA) *m/z* = 183 (100 %, $[MH]^+$), 152 (43 %, $[MH-CH_3N]^+$), 136 (18 %, $[MH-CH_3NO]^+$).

[Eu(TREN-1,2-HOPO)(H_2O)]$_2$:

To a solution of TREN-1,2-HOPO (61 mg, 0.10 mmol) in methanol (10 mL), was added a solution of europium chloride hexahydrate (36 mg, 0.1 mmol) in methanol (10 mL) while stirring. The clear solution became turbid after 2 drops of dry pyridine were added. The mixture was refluxed overnight under nitrogen, during which time the complex deposited as a white powder. The precipitate was

collected, rinsed with cold methanol, and dried to give the title complex (63 mg, 89 %) as a white solid. Anal. for $EuC_{24}H_{24}N_7O_9 \cdot H_2O$, Calcd. (Found): C, 39.79 (40.01); H, 3.62 (3.47); N, 13.53 (13.26).

Crystals of $[Eu(C_{24}H_{24}N_7O_9 \cdot C_3H_7NO)]_2$ x 0.5 C_3H_7NO x 0.5 $C_4H_{10}O$ suitable for X-ray diffraction were obtained from vapor diffusion of diethyl ether into a DMF solution (Table S1).

Solution Thermodynamics

The experimental protocols and equipment used have been previously described.[16] To determine the protonation constants of the free ligand, approximately 13.5 to 25.2 mg of ligand was dissolved in 25 or 50 mL of a 0.1 M aqueous solution of KCl in a titration vessel (ligand concentration ~0.4 to 0.7 mM). Protonation constants of TREN-1,2-HOPO were determined by potentiometric (pH vs total proton concentration) titrations using Hyperquad[17] for data refinement. Each protonation constant determination is the result of at least three experiments (where each experiment consists of two titrations, the first one titrated with acid, followed by a reverse titration with base). The equilibration time between additions of titrant was 90 seconds for ligand titrations. Spectrophotometric titrations of ~40 μmol solutions of TREN-1,2-HOPO were fitted using pHAb[18] for computation. Molar absorbances of the species L^{3-}, LH^{2-}, LH_2^-, LH_3, and LH_4^+ were determined (Figure S3) and interpreted to assign protonation sites. The smallest change in absorption between two species results from the protonation at the amine nitrogen atom, which is not directly adjacent to the 1,2-HOPO chromophores monitored in the wavelength region between 280 and 380 nm.

^1H (Table S6; Figure 4) and ^{13}C NMR (Table S7; Figure S3) titrations were performed on a solution of TREN-1,2-HOPO (88.34 mM) in 4 mL D_2O. The pD of this solution was also monitored and varied by stepwise addition of KOD/D_2O (30 %; ~1–10 μL). The corresponding pH was calculated by the relation pD = 1.044 pH – 0.32.[19] A small amount of methanol was used as standard (δ^{1H} = 3.32 ppm; δ^{13C} = 49.50 ppm).[20]

The general procedure used to determine the conditional stability constants pGd, pZn or pCa of a TREN-1,2-HOPO complex was competition batch titration adapted from a previous report.[21] Varying volumes of a standardized DTPA stock solution were added to solutions containing constant ligand, metal, buffer [0.01 M of either MES (= 2-(N-morpholine)-ethanesulfonic acid) pH 6.1; HEPES (= 4-(2-hydroxyethyl)-1-piperazineethanesulfonic acid) or TRIS (= 2-amino-2-hydroxymethyl-propane-1,3-diol) for pH 7.4] and electrolyte (0.1 M KCl) concentrations. If necessary, the pH of the solutions was adjusted with concentrated HCl and/or KOH and the solutions were diluted to identical volumes in buffered electrolyte solution. The concentrations of TREN-1,2-HOPO relative to DTPA ranged from 10:1 to 1:1000. After equilibrating for 24 h to ensure thermodynamic equilibrium, concentrations of free and complexed TREN-1,2-HOPO were determined from the absorption spectra, using the wavelength range from 320 – 360 nm (pGd; Figures 5 and S7), 320 – 350 nm (pZn; Figures 7 and S8), 320 – 350 nm (pCa; Figure S9) and the spectra of free and fully complexed TREN-1,2-HOPO as references.

Photophysical Measurements

UV-Visible absorption spectra were recorded on a Varian Cary 300 double beam absorption spectrometer using quartz cells of 1.00 cm path length. Emission spectra were acquired on a HORIBA Jobin Yvon IBH FluoroLog-3 spectrofluorimeter, equipped with 3 slit double grating excitation & emission monochromators (2.1 nm/mm dispersion, 1200 grooves/mm). Spectra were reference corrected for both the excitation light source variation (lamp and grating) and the emission spectral response (detector and grating).

Luminescence lifetimes were determined on a HORIBA Jobin Yvon IBH FluoroLog-3 spectrofluorimeter, adapted for time-correlated single photon counting (TCSPC) and multichannel scaling (MCS) measurements. A sub-microsecond Xenon flashlamp (Jobin Yvon, 5000XeF) was used as the light source, with an input pulse energy (100 nF discharge capacitance) of *ca*. 50 mJ, yielding an optical pulse duration of less than 300 ns at FWHM. Spectral selection was achieved by passage through a double grating excitation monochromator (2.1 nm/mm dispersion, 1200 grooves/mm).

Emission was monitored perpendicular to the excitation pulse, again with spectral selection achieved by passage through a double grating excitation monochromator (2.1 nm/mm dispersion, 1200 grooves/mm). A thermoelectrically cooled single photon detection module (HORIBA Jobin Yvon IBH, TBX-04-D) incorporating fast rise time PMT, wide bandwidth pre-amplifier and picosecond constant fraction discriminator was used as the detector. Signals were acquired using an IBH DataStation Hub photon counting module and data analysis was performed using the commercially available DAS 6 decay analysis software package from HORIBA Jobin Yvon IBH. Goodness of fit was assessed by minimizing the reduced chi squared function, χ^2, and a visual inspection of the weighted residuals. Each trace contained 10,000 points and the reported lifetime values result from three independent measurements. Typical sample concentrations for both absorption and fluorescence measurements were *ca*. 10^{-5}-10^{-6} M and 1.0 cm cells in quartz suprasil or equivalent were used for all measurements. An example of a typical lifetime data trace and the corresponding best fit is shown in Figure S1.

Relaxometric Measurements

The water proton $1/T_1$ longitudinal relaxation rates (20 MHz, 25°C) were measured on a Stelar Spinmaster Spectrometer (Mede, Pv, Italy) on 30-45 μM aqueous solutions of the complexes. For the T_1 determinations the standard inversion-recovery method was used with typical 90° pulse width of 3.5 μs, 16 experiments of 4 scans. The reproducibility of the T_1 data was estimated to be ±1%. The temperature was controlled with a Stelar VTC-91 air-flow heater equipped with a copper-constantan thermocouple (uncertainty of 0.1±°C). In a typical titration experiment several (5-8) aqueous solutions at pH = 6.0 of the paramagnetic complex were prepared containing different concentrations of the anionic species (0-0.04 M) and the water proton relaxation rate of each solution was measured at 25°C. The starting pH was adjusted by either HCl or KOH. Moreover, the pH of the solutions was controlled before and after the measurement.

Results and Discussion

Solid State Structure

The Eu(III) complex of TREN-1,2-HOPO (Figure 1) is isostructural with the Gd(III) complex. Both complexes crystallize in the monoclinic space group P2/n in dinuclear units, linked via an amide carbonyl oxygen atom and the lanthanide of the adjacent complex. Each ligand coordinates one metal center in a hexadentate fashion with a single DMF molecule completing the coordination sphere of the metal to eight (CN = 8). Distances for Ln-O bonds vary only to a very small degree reflecting the lanthanide contraction. Also the geometry around Gd(III) and Eu(III) atoms is identical as determined by the shape measure S[22] for eight coordinate metal centers (Table S2) according to Kepert.[23] The coordination geometry is described best by C_{2v} symmetry corresponding to a bicapped trigonal prism.

Solution Structure

In aqueous solution, the amide oxygen atoms of DMF and the adjacent ligand are replaced with two fast exchanging water molecules (q = 2) as suggested by the NMRD profiles.[15] For the first time, the number of coordinated water molecules q of a TREN-HOPO chelate could also be confirmed by luminescence spectroscopy of its parent Eu(III) complex. The luminescence quenching of coordinated water molecules can be used to determine q directly.[13] Luminescence decaytimes of the Eu-TREN-1,2-HOPO complex were found to be monoexponential at pH ~ 6 in aqueous solution and in D_2O, with lifetimes of 222 μsec and 372 μsec, respectively (Figure S1). Utilizing the improved Horrocks relationship given by Parker[24] gave an estimate of q = 1.9, which confirms the results obtained for the Gd(III) complex via relaxivity.

For Eu(III), the $^5D_0 \rightarrow {}^7F_J$ transitions are amenable to structural interpretation since, depending on the symmetry, crystal field splitting yields a maximum of 2J + 1 sublevels. Hence, emission spectra of the complex will reflect the symmetry of its immediate surroundings,[25] and a complete analysis of crystal

field splitting parameters for the Eu(III) ion under various symmetry conditions using the principles of group theory has been detailed in the literature (Table S3).[26]

Given the determination of an overall eight coordinate ($q = 2$) complex, a closer analysis of the emission spectra, in particular for the $^5D_0 \rightarrow {}^7F_J$ (J = 0, 1) transitions, reveals insight into the solution behavior of the Eu(III) complex (Figure 2). The strength of the intensity of the J = 0 band at *ca.* 17,300 cm^{-1} is comparable to J = 1 bands, which suggests this transition is symmetry allowed, implying C_{2v} symmetry. Further analysis for the J = 1 region (*ca.* 16,700 cm^{-1} to 17, 100 cm^{-1}) confirms this assignment since only under C_{2v} symmetry are three J = 1 bands expected, as clearly observed in the spectral deconvolution. Hence, the site symmetry C_{2v} observed by X-ray crystallography for the TREN derivative is maintained in solution.

Ligand Protonation

Ligand protonation constants were determined by potentiometry in 0.1 M KCl (Table 1). Spectrophotometric and NMR titrations confirm these pK_a values (Table S5). At physiological pH the ligand is almost completely deprotonated and available for metal complexation (Figure S2). The protonation sites have been assigned based on the molar absorbances of the species fitting spectrophotometric titrations (Figure 3). The very similar absorbances of the two most basic species (HL^{2-} and L^{3-}) indicate that the most basic protonation constant pK_a 7.16 (1) should be assigned to the tertiary amine, since this protonation site is not directly linked to the 1,2-HOPO chromophores monitored between 260 and 400 nm. This assignment is supported by ^1H and ^{13}C NMR titrations (Figures 4 and S3, Tables S4–S6). In addition, assignment of resonances in ^1H and ^{13}C NMR spectra based on two dimensional HMBC and HMQC (Figures S4–6) spectra gave insight into molecular processes involved with protonation. While only minor shifts are observed for the aromatic proton resonances, the signals for 1´-CH_2 and 5-CH (Chart 2) are shifting significantly between pH 5.3 and 7.7. The influence of deprotonation of the tertiary amine on the 1´-CH_2 protons is clear, however, the reason

for the change in 5-CH resonance indicates that the structure of the molecule changes significantly. A careful analysis of shifts in proton and carbon resonances corroborates the hypothesis that the molecular solution structure of TREN-1,2-HOPO changes upon deprotonation by 180° rearrangement around the bond between 2´-CH_2 and the amide nitrogen (Scheme 1) to maximize stabilizing hydrogen bond interactions.

The average of the three pK_a values associated with 1,2-HOPO hydroxylgroups ($pK_{a\,av} = 4.52$) is slightly more acidic than expected based on similar compounds such as propyl-1,2-HOPO (pK_a = 4.92).[27] Also in contrast to 1-Me-3,2-HOPO-TREN (pK_a = 4.97) or the model compound TREN-MeSAM (pK_a = 6.01 (7))[28] the tertiary amine is more basic (pK_a = 7.16 (1)). This can be rationalized by the hydrogen bond network, which links the four protonation sites via the amide hydrogen atoms and by electrostatic interaction caused by additional charges in TREN-1,2-HOPO. Protonation constants of model compounds Pr-3,2-HOPO (pK_a = 6.12 (1)), Pr-1,2-HOPO (pK_a = 4.92 (2)) and TREN-MeSAM (pK_a = 6.01 (7)) support this assignment and illustrate the difference in the acidity of protonation sites of TREN-1,2-HOPO and TREN-3,2-HOPO. The interaction between the protonation sites amplifies effects resulting from deprotonation at adjacent sites, which change the pK_a values. Thus, the pK_a values in both TREN-3,2-HOPO and TREN-1,2-HOPO are lower for the more acidic and higher for the more basic moieties compared to reference compounds. The "undisturbed" tertiary amine has a pK_a 6.01 (7), which is more acidic than the 3,2-HOPO hydroxyl group, but more basic than the 1,2-HOPO hydroxyl group. This reverse assignment of protonation sites of TREN-1,2-HOPO (amine most basic pK_a = 7.16) compared to TREN-3,2-HOPO (amine most acidic pK_a = 4.97) is important for explaining differences in the lanthanide chelation and protonation behavior (*vide infra*).

Stability of the Gadolinium Complex

The low solubility of [Gd(TREN-1,2-HOPO)(H_2O)$_2$] (c_{sat} = 85 μM) prevents potentiometric titrations for stability assessment and automated spectrophotometric titration experiments were prevented by slow

protonation kinetics. Hysteresis behavior for the titration from acidic to basic pH and reverse was observed between pH 4 and 8. Notably, no protonation is observed above pH 8 since the tertiary amine represents the most basic function in the ligand. We assign the tertiary amine of the TREN scaffold as also the most basic function in this ligand. The observed slow equilibration we attribute to slowed rotation in the ligand around the CC bond between carbamide and aryl ring, most likely occurring upon change of the protonation state at the tertiary amine. It has been shown previously for similar ligands that the resulting hydrogen bond network for the protonated ligand and the metal complex results in different conformations.[29] The fact that this kinetic hindrance is not observed for TREN-3,2-HOPO and similar more basic ligands corroborates the assumption that the amine protonation is crucial for this behavior.

Slow kinetics were circumvented by using batch titration techniques, which allow for long equilibration times typically between one and three days. Competition batch titrations versus DTPA were employed to determine the conditional stability constants at pH 6.1 and 7.4 (Figure 5). From these data and the protonation constants of the ligand, the Gd(III) complex formation constant $\log\beta_{110}$ 18.5 (2) was calculated. This number and the protonation of the complex at pK_a 5.0 (2) and 3.5 (5) are reflected in changes of fluorescence intensity versus pH of the Eu(III) complex (Figure S10) and relaxivity versus pH of the Gd(III) complex (Figure S11). In the alkaline region TREN-1,2-HOPO competes with the formation of europium hydroxide.[30] The competition of oxide formation at high pH is accurately modeled using $\log\beta_{110}$ 18.0 (5) and published europium oxide formation constants. In addition the pH profile of relaxivity suggests that Gd(III) remains coordinated to very acidic pH values, around 1. This is in agreement with the suggested stability and the acidic nature of TREN-1,2-HOPO. Consequently, a non- or only very weakly luminescent species is formed upon first complex protonation. The increase in relaxivity from pH 4 to 2 is caused by partial hydrolysis of one ligand arm from a doubly protonated complex. While the site of the first complex protonation is attributed to the scaffold amine, which is the most basic function in the complex, the second protonation removes one of the 1,2-HOPO groups

leaving space for two additional water molecules. The increase in relaxivity from 9.5 to 17 $mM^{-1}s^{-1}$ reflects this doubling of water coordination sites.

The $pGd^{7.4}$ 19.3 (2) of TREN-1,2-HOPO is remarkably high considering the acidity of this ligand. A comparison of conditional stability constants pGd of TREN-3,2-HOPO, DTPA and TREN-1,2-HOPO versus pH demonstrates the advantage of TREN-1,2-HOPO (Figure 6). pGd reaches an optimum value at pH values at which ligand deprotonation no longer plays a role in the complexation equilibrium. Thus, for basic ligands such as DTPA or TREN-3,2-HOPO, deprotonation still limits the conditional stability constant pGd at pH 7.4 compared to logβ. By contrast, the more acidic TREN-1,2-HOPO reaches the "plateau" resulting from complete ligand deprotonation around physiological pH. Importantly, for application in MRI pH values above 7.4 play only a minor role. In contrast, acidotic patients with renal failure undergoing imaging have been reported to acquire symptoms of Gd(III) poisoning.[31] A more acidic ligand such as TREN-1,2-HOPO clearly provides increased stability in the region between pH 1 and 7.

Selectivity for Gd(III) versus Zn(II) and Ca(II)

The toxicity of a MRI-CA does not only correlate with its thermodynamic complex stability, but also with metal binding selectivity of the ligand. Thus, the high gadolinium complex stability of a TREN-1,2-HOPO needs to be completed by either very slow kinetics for metal exchange or preferably by maximized thermodynamic selectivity for Gd(III) over endogenous metals to prevent Gd(III) release *in vivo*. Zn(II) and Ca(II) are the most abundant metals in this respect, since the concentrations of uncomplexed Zn(II) (10-15 μM) and Ca(II) (0.4 – 2.5 mM) in serum are sufficient for release of lethal amounts of Gd(III) (~20 μM).[1] The selectivity of TREN-1,2-HOPO for Gd(III) over Zn(II) and Ca(II) was determined by comparing the conditional stability constants pGd and pZn or pCa with those for the benchmark compound DTPA (pGd-pZn = 4.2; pGd-pCa = 11.7).

Competition batch titrations against DTPA were employed to obtain complex stabilities for Zn(II)-TREN-1,2-HOPO (Table 1, Figure 7). The competition experiments were performed at pH 6.1 and 7.4. Contrary to the Gd(III) chelate, no protonation occurs between pH 4.5 and 9. From these competition experiments pZn 15.2 (2) and $\log\beta_{110}$ 14.4 (1) were calculated. The Zn(II) binding of TREN-1,2-HOPO is relatively strong compared to bidentate 1,2-hydroxypyridinone, which forms a quaternary complex ZnL_3 with $\log\beta_{130}$ 11.99.[32] This increase in stability for TREN-1,2-HOPO may be attributed to involvement of the amine nitrogen atom in binding Zn(II), which also might account for the lack of observed amine protonation. The selectivity of TREN-1,2-HOPO for Gd(III) chelation over Zn(II) measured by the difference in conditional stability constants pGd-pZn 4.1 is sufficient compared to DTPA with pGd-pZn 4.2.

Competition batch titrations of TREN-1,2-HOPO versus DTPA for Ca(II) resulted in $pCa^{7.4}$ 8.8 (3) (Figure S9). While more stable than Ca-DTPA, this low stability allows formation of Ca-TREN-1,2-HOPO only above pH 4 in the presence of physiological amounts of Ca(II) (2.5 mM). The selectivity of TREN-1,2-HOPO versus Ca(II) pCa-pGd 10.5 is excellent.

3,2-HOPO ligands that form anionic and cationic Gd(III)chelates are highly selective for Gd(III) over Ca(II) and Zn(II) with ΔpM (Gd-Zn) between 6 and 8.[33] Comparing basic 3,2-HOPO with acidic 1,2-HOPO ligands, Zn(II) binding increases for more acidic ligands, while Gd(III) binding decreases for such ligands. Thus, for the design of highly selective and acid resistant MRI-CA, mixed ligands of acidic 1,2-HOPO and more basic 3,2-HOPO groups are suggested. Alternately, the number of acidic chelate groups could be raised to four resulting in an octadentate ligand with preferential binding of lanthanides.[1]

Anion Affinity

Anion binding at the water coordination site reduces the efficiency of a MRI-CA by replacing these water molecules. For aminocarboxylate ligands, anion binding has been studied with a chiral macrocycle by luminescence spectroscopy of the Eu(III) complex, relaxometry of Gd(III) chelates, and NMR spectroscopy of Yb(III) complexes. In addition solid state crystal structures of ternary complexes were obtained to correlate solid and proposed solution structures.[34] Binding constants of phosphate and oxalate are relatively low for DOTA and DTPA, but cationic complexes of DO3A amide derivatives ($q = 2$) can efficiently bind bidentate carboxylates such as citrate or malonate.[35] Unlike these cationic chelates, neutral 3,2-HOPO complexes with $q = 2$ do not or only weakly bind biorelevant anions. Also a cationic and an anionic bis-3,2-HOPO-TAM chelate show smaller association constants with phosphate and oxalate than the commercial, $q = 1$ chelates Gd(DOTA) or Gd(DTPA).[33]

The affinity of Ln-TREN-1,2-HOPO towards several anions was evaluated by relaxometry of the Gd(III) complex and luminescence spectrosocopy of the Eu(III) complex (Table 2). Endogenous anions like phosphate, carbonate, acetate, or malonate do not interact with both complexes (Figure 8). A weak interaction with oxalate was detected by decreasing relaxation rate (Figure 9) and increasing luminescence intensity. For complete formation of the ternary complex 1500 equivalents of oxalate are required, which corresponds to a very small binding constant of K_a 82.7 ± 6.5 M^{-1} for the Gd(III) complex and 96 M^{-1} for the Eu(III) complex.

Ascorbate and catecholate decrease the luminescence intensity of the Eu(III) complex, but no interaction was observed by relaxometry indicating the mechanism for luminescence quenching of the Eu(III) complex does not involve coordination at the metal center. It is possible the ligand triplet state may be quenched by catechol or ascorbate, or alternately, the excited Eu(III) may be partially reduced to Eu(II), which is too high in energy for sensitization by TREN-1,2-HOPO.

It was also noted that the addition of up to 1000 equivalents of fluoride did not replace water. The only strong binding interaction was observed for a bidentate 3,2-HOPO anion (Figure 9). The binding constant is within the expected value around 3100 M^{-1} ($\log K_a$ 3.5). This observation corroborates the assumption that only monoanionic and bidentate ligands would form strong ternary complexes with Eu-TREN-1,2-HOPO. The 3,2-HOPO anion binds 1.5 order of magnitude stronger than oxalate, with saturation already below 20 equivalents while other bidentate ligands like catechol or maltol do not bind.

Solution Structure of Ternary Complexes

The change of relaxation rates between Gd-TREN-1,2-HOPO and the ternary adducts suggests that the coordination number increases from 8 to 9 upon binding of bidentate 3,2-HOPO or oxalate (Figure 10). Indeed, the calculated relaxivities r_{1p} (20 MHz, 25°C) of the ternary complexes (Table 2) are 5.5±0.2 and 5.2±0.2 $mM^{-1}\ s^{-1}$. These are typical values for q = 1 complexes. Pure outer sphere complexes (q = 0) would be characterized by relaxivity values of ca. 2.5-3.0 $mM^{-1}\ s^{-1}$ under identical experimental conditions.

Titrations of the Eu(III) complex with oxalate were monitored by variation of luminescence decay lifetimes which rise from 220 μs to 332 μs upon addition of 1500 equivalents of potassium oxalate. Under these conditions the ternary complex is the dominant species, which is also recognized by slight changes in the emission spectrum. Lifetime measurements clearly indicated the new species has one coordinated water (q = 0.8).[24] The fact that ligands with one carboxylate group do not coordinate under these experimental conditions corroborates that oxalate functions as a bidentate ligand replacing only one water molecule. Such behavior was observed earlier in the oxalate binding of a tren substituted bis-3,2,-HOPO-TAM-TREN complex, which was interpreted as shifting the equilibrium from 8 and 9 coordinate complexes upon addition of oxalate.[33] The emission spectrum of a 10 μM Eu-TREN-1,2-HOPO solution with 1500 equivalents oxalate differs slightly from the one of

a pure Eu-TREN-1,2-HOPO solution. Symmetry analysis of the J = 0 and 1 bands (Figure 10) for a nine-coordinate Eu(III) center suggests that the coordination geometry is a subgroup of C_{4v}, since otherwise the J = 0 band would be absent (Table S3). Fitting the J = 1 band with three equally broad and intense Voigt functions (A and 2B) provides better a result than with two Voigt functions of a 2:1 intensity ratio (A and E). Thus the coordination geometry at the metal center can be assigned to C_2, a subgroup of C_{4V}.

Conclusion

The X-ray structures of [Eu(TREN-1,2-HOPO)(H_2O)$_2$] and [Gd(TREN-1,2-HOPO)(H_2O)$_2$] are isostructural with identical coordination geometries at the metal centers. This allows the direct comparison of relaxometric measurements of the Gd(III) complex with the emission spectra of the Eu(III) complex. The protonation constants of TREN-1,2-HOPO were determined and assigned revealing a change in the order of protonation sites, which also influences the sequence of protonating the Gd(III) complex. The high Gd(III) binding constant of TREN-1,2-HOPO is matched by sufficient selectivity versus Zn(II) and excellent selectivity versus Ca(II) binding. In addition, the greater ligand acidity provides enhanced stability under slightly acidic conditions. The expectation of low toxicity Gd(III)-TREN-1,2-HOPO is completed by low anion interactions. A detailed study on the ternary oxalate adduct reveals insights into solution structure and demonstrates the comparable energies of the 8- and 9 coordinate Gd(III), which is an essential feature for the advantageous relaxometric properties of the MRI contrast agents based on HOPO chelates.

Despite the differences, 1,2-HOPO chelates overall serve as good models for non-luminescent 3,2-HOPO chelates. The higher acidity of the 1,2-HOPO chelate group compared to 3,2-HOPO facilitates handling and analysis since the complexes are less sensitive to acid hydrolysis. The advantages of using 1,2-HOPO over 3,2-HOPO are the lower anion affinity, higher acid resistance of the lanthanide chelate

and the utilization of Eu(III) luminescence to reveal information on the solution structure. Further research aims on improving the water solubility of 1,2-HOPO derivatives.[36]

ACKNOWLEDGMENT. This work (UCB) was supported by NIH Grant HL69832, by the Director, Office of Science, Office of Advanced Scientific Computing Research, Office of Basic Energy Sciences (U.S. Department of Energy) under contract DE-AC02-05CH11231 and NATO travel grant PST.CLG.980380. CJJ acknowledges the German Research Foundation (DFG) for a postdoctoral fellowship. Support from MIUR (COFIN 2005) is also gratefully acknowledged (M.B., S.A.). The authors acknowledge Eric Werner for helpful discussions and proof reading of the manuscript.

Supporting Information Available: Single crystal X-ray diffraction data (CIF) and additional tables (symmetry analysis and titration refinements) and figures (2D NMR data, titration data, pH-luminescence profile, pH relaxivity profile) as pdf file. This material is available free of charge via the Internet at http://pubs.acs.org.

Chart 1. 1,2-HOPO, 3,2-HOPO and TAM chelates are used to prepare stable Gd(III) complexes as MRI contrast agents.

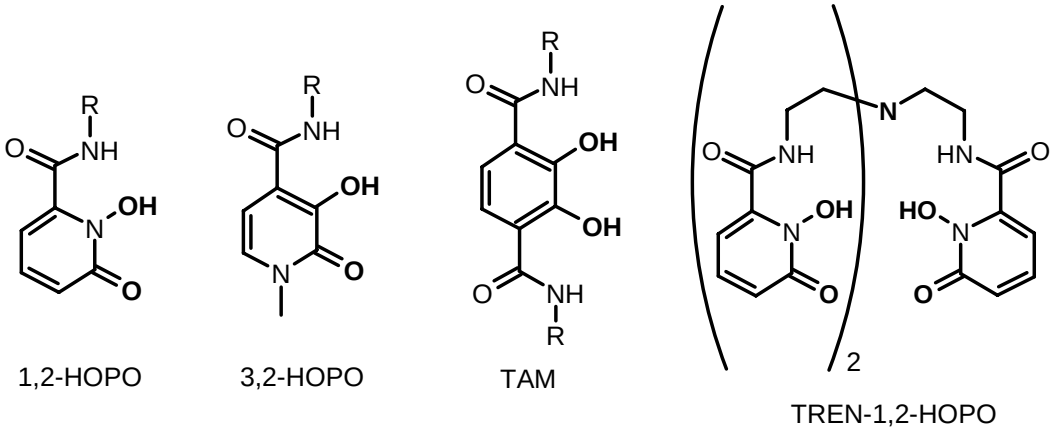

Chart 2. TREN-1,2-HOPO and labeling scheme used to assign the ^{1}H (Figure 4) and ^{13}C NMR spectra.

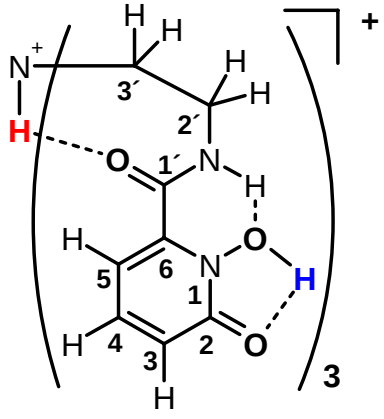

Figure 1. Ortep plot (50 % probability) of [Eu(TREN-1,2-HOPO)(DMF)]$_2$. Non-coordinating solvent molecules and hydrogen atoms have been omitted. Selected bond lengths (Å) and angles (deg): Eu1-O1a 2.389(4); Eu1-O2a 2.387(4); Eu1-O1b 2.360(4); Eu1-O2b 2.366(4); Eu1-O1c 2.407(4); Eu1-O2c 2.379(4); Eu1-O1s1 2.396(4); Eu1-O3c* 2.467(4); Eu1-O1b-N1b 119.2(3); O1b-N1b-C1b 115.9(5); Eu1-O2b-C1b 123.0(4); N1b-C1b-O2b 116.1(5); O1b-Eu1-O2b 64.73(14); Eu1-O3c*-C6c* 125.8(4). (*) and (_3) indicate symmetry generated atoms.

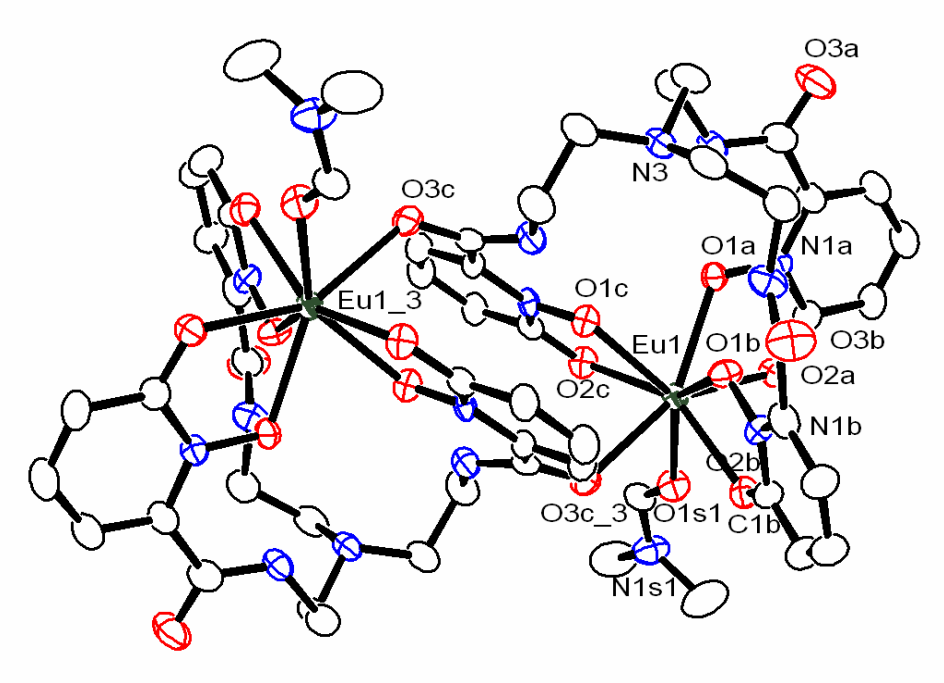

Figure 2. The emission spectrum of a [Eu(TREN-1,2-HOPO)(H_2O)$_2$] in aqueous solution at pH 6. The inset shows the expansion of emission spectra in the $^5D_0 \rightarrow {}^7F_J$ (J = 0, 1; 570 to 600 nm) region and corresponding spectral deconvolution into several overlapping Voigt functions.

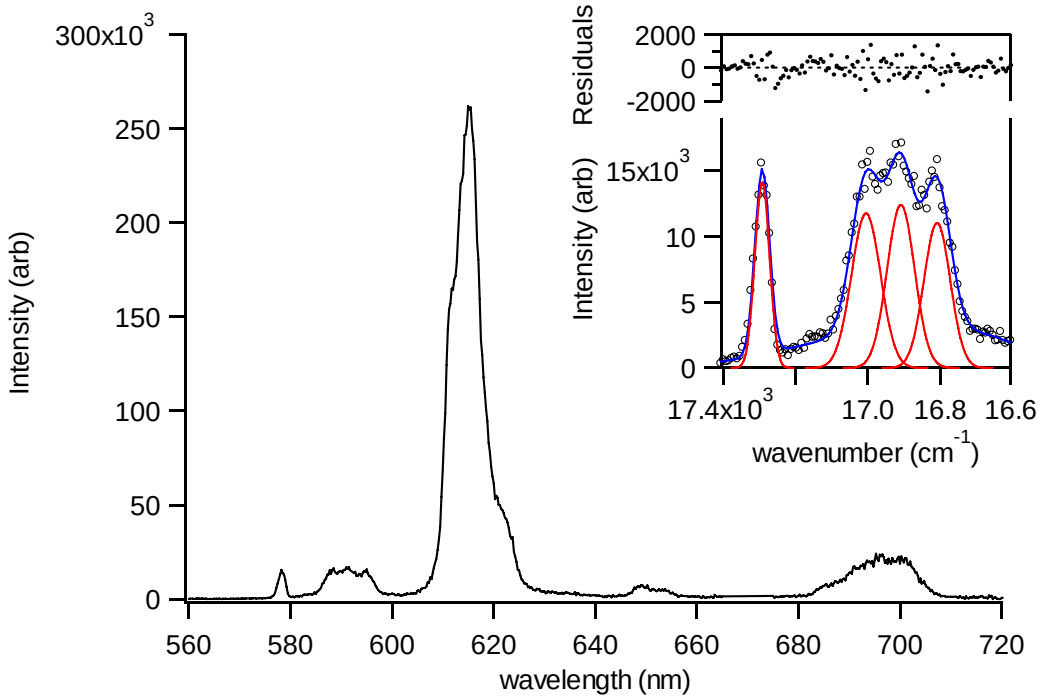

Figure 3. Left: Spectrophotometric titration of TREN-1,2-HOPO. Right: Fitted molar absorbances for the five protonation states of TREN-1,2-HOPO.

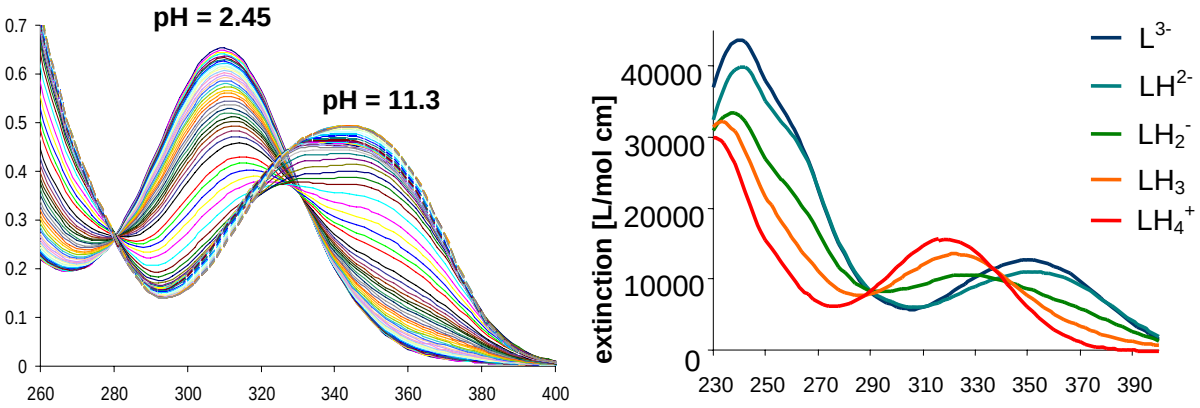

Figure 4. ^{1}H NMR titration of TREN-1,2-HOPO from pH 1.11 to 8.93 in D_2O. The labeling scheme is depicted in Chart 2.

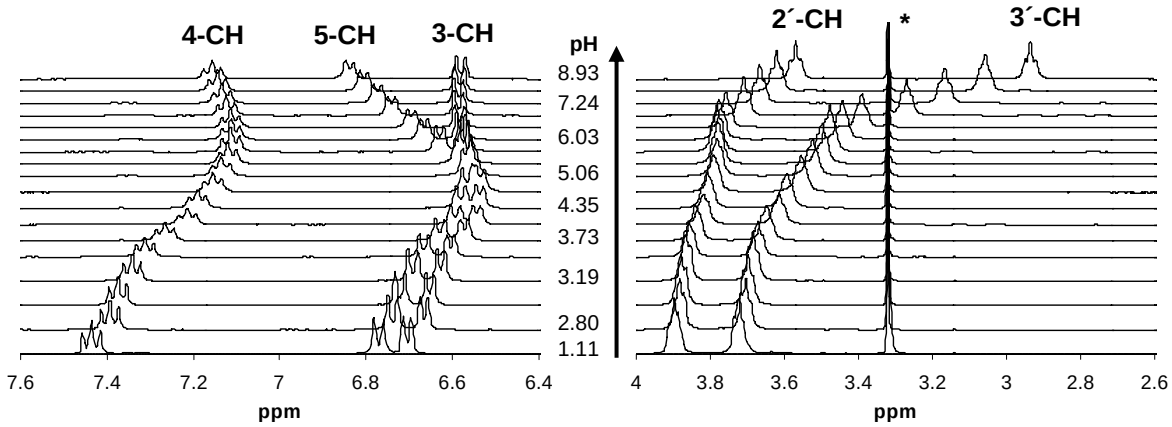

* trace of methanol for calibration.

Figure 5. Left: Obtained spectra for the competition batch titration of TREN-1,2-HOPO versus DTPA for Gd(III) complexation at pH 7.4 in 0.1 M KCl solution. The blue line marks the spectrum of Gd-TREN-1,2-HOPO, the red line is uncomplexed ligand and between are spectra obtained by addition of up to 85 equivalents of DTPA. Right: double logarithmic plot of concentration ratios (at equilibrium; after 24 hrs.) for determination of the conditional stability constant $pGd^{7.4}$ 19.3 (2).

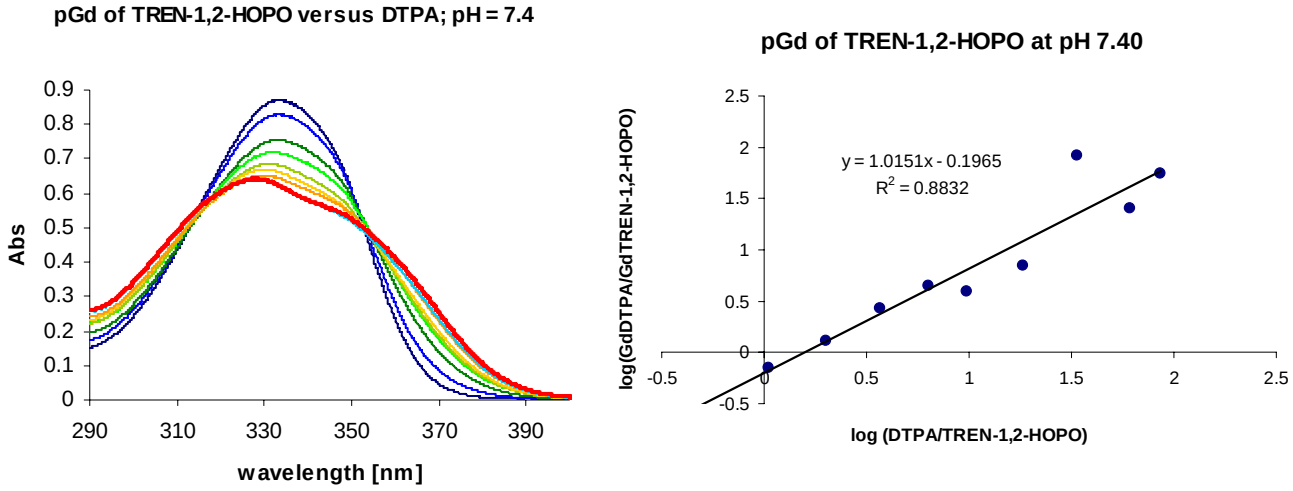

Figure 6. Comparison of conditional stability constant (pGd) of TREN-1,2-HOPO (blue) with DTPA (red) and TREN-3,2-HOPO (green) at variable pH.

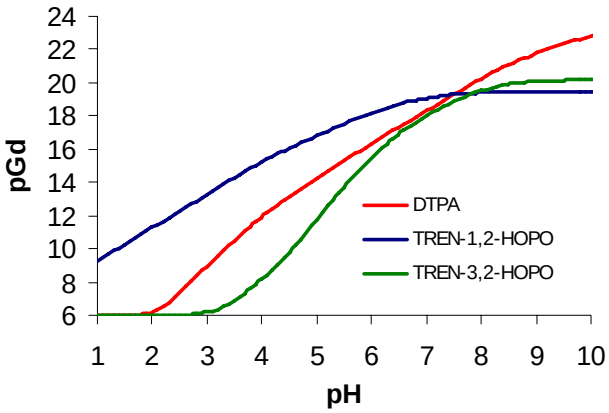

Figure 7. Left: obtained spectra for the competition batch titration of TREN-1,2-HOPO versus DTPA for Zn(II) complexation at pH 7.4 in 0.1 M KCl solution. The blue line marks the spectrum of Zn-TREN-1,2-HOPO and the red line Zn-TREN-1,2-HOPO with 20 equivalents of DTPA. Right: double logarithmic plot of concentration ratios (at equilibrium; after 24 hrs.) for determination of the conditional stability constant $pZn^{7.4}$ 15.2 (2).

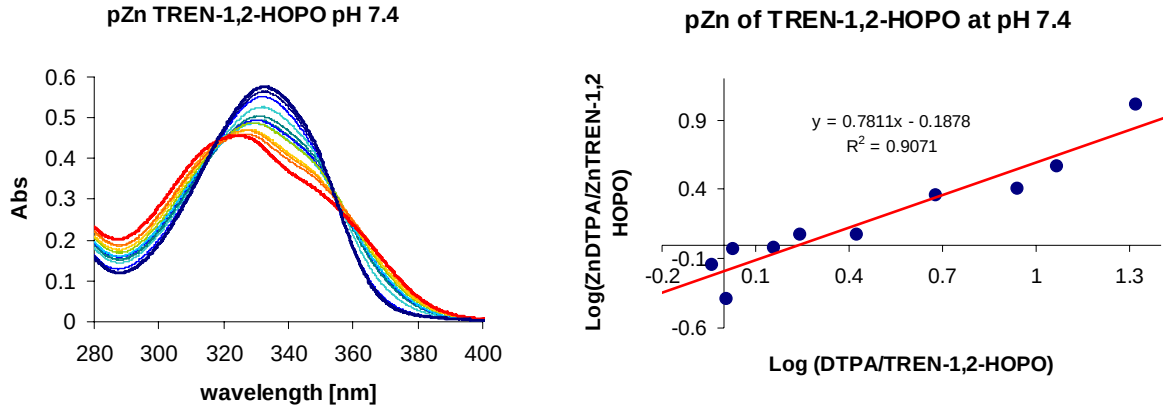

Figure 8. Observed changes in luminescence of a 10 μM solution of [Eu(TREN-1,2-HOPO)] at pH 6 upon titration with concentrated solutions of several biologically relevant anions.

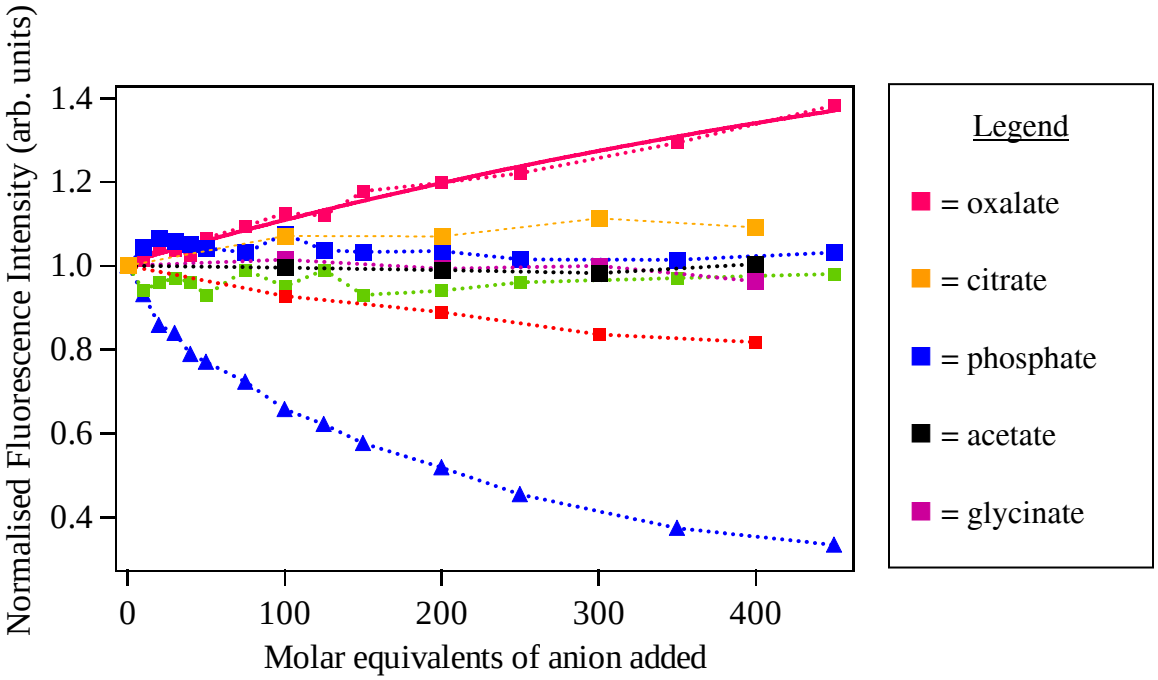

Figure 9. Relaxometric determination of the association constants K_A for oxalate (left) and a bidentate 3,2-HOPO ligand (right) with Gd-TREN-1,2-HOPO (c = 35 µmol; 20 MHz; 25 C).

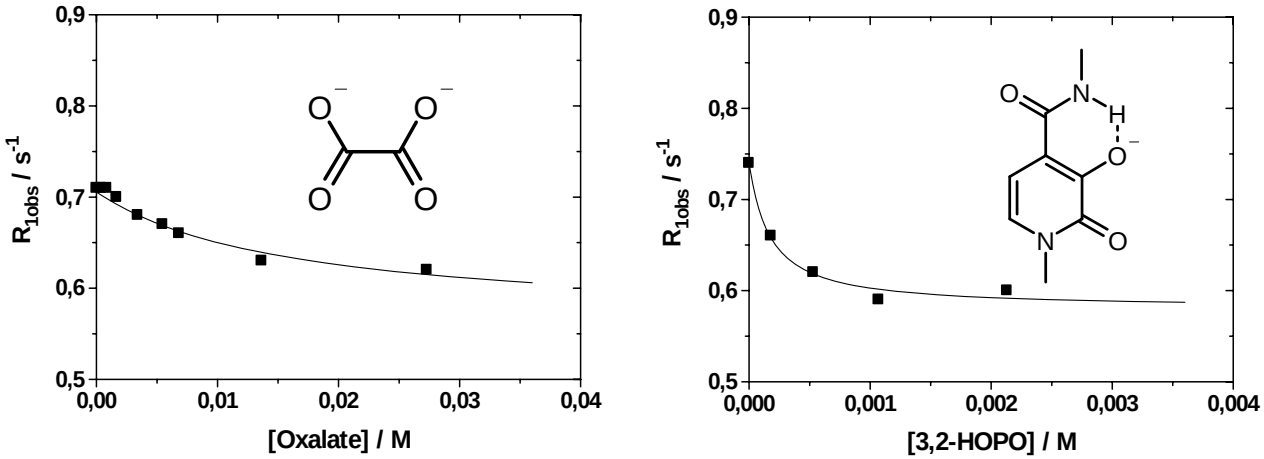

Figure 10. Observed emission spectrum for the oxalate (c = 15 mM) adduct of [Eu(TREN-1,2-HOPO)(H_2O)$_2$] (c = 10 μM) in aqueous solution at pH 6. The inset shows the expansion of emission spectra in the $^5D_0 \rightarrow {}^7F_J$ (J = 0, 1; 570 to 600 nm) region and corresponding spectral deconvolution into several overlapping Voigt functions.

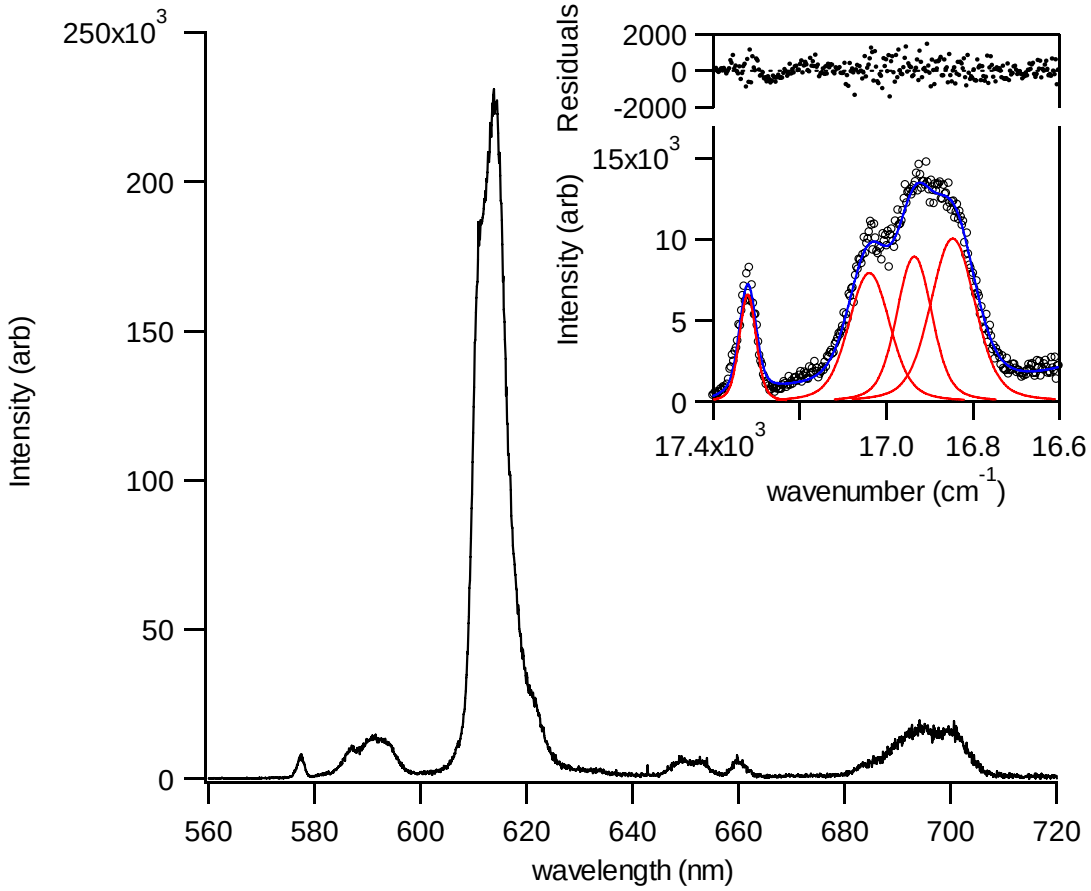

Scheme 1. Structural changes associated with the deprotonation of TREN-1,2-HOPO. The deprotonation of the hydoxylgroups (blue) does not change the hydrogen bonding pattern. The loss of hydrogen bonding interaction by removing the proton from the tertiary amine (red) is compensated by interaction of the lone pair of the resulting amine with amide protons.

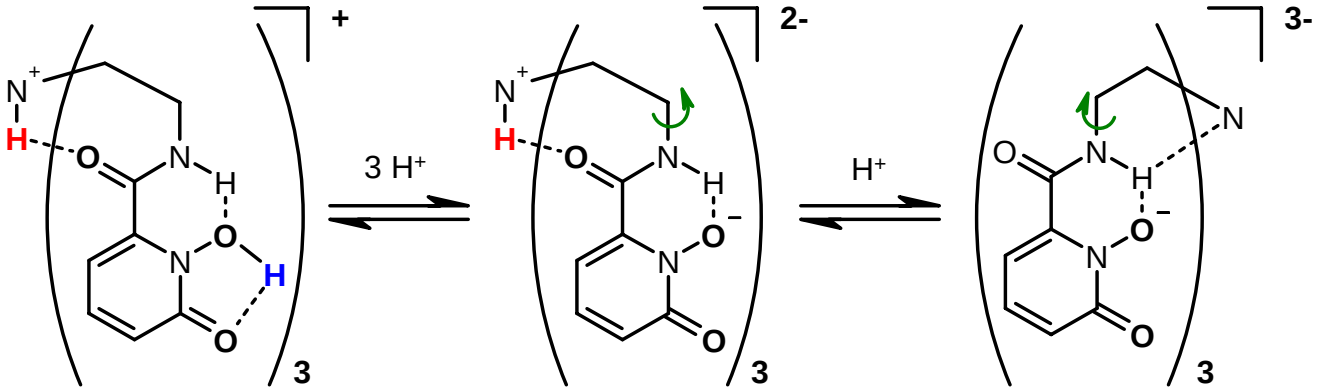

Scheme 2. Oxalate binding of Gd-TREN-1,2-HOPO. One oxalate anion bound in a bidentate fashion replaces one water molecule increasing the coordination number at Gd(III) from 8 to 9. This illustrates the small difference in energy between the eight and nine coordinate geometries.

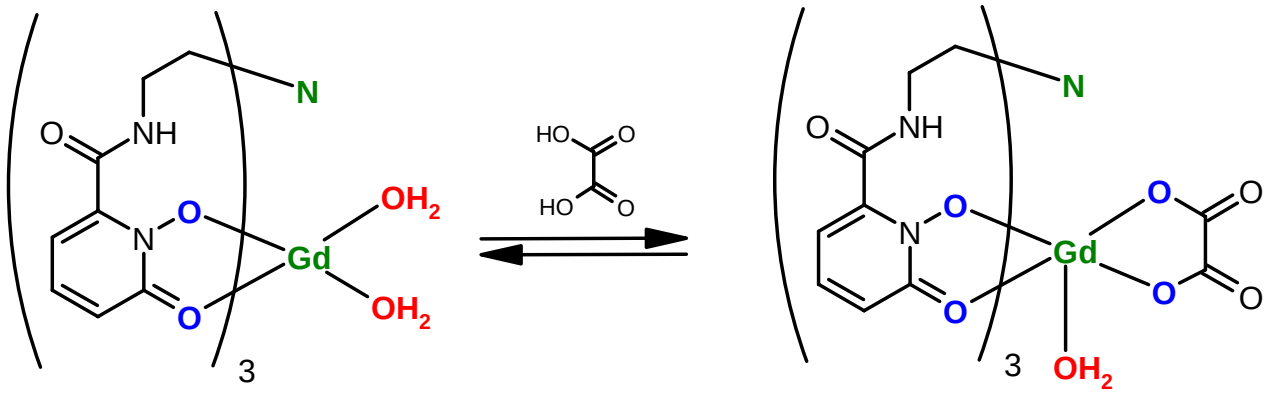

Table 1. Solution thermodynamic constants of TREN-1,2-HOPO.

	logβ	pK_a
$L^{3-} \leftrightarrows HL^{2-}$	7.16 (1)	7.16 (1)
$HL^{2-} \leftrightarrows H_2L^{-}$	12.78 (2)	5.62 (2)
$H_2L^{-} \leftrightarrows H_3L$	17.10 (3)	4.32 (3)
$H_3L \leftrightarrows H_4L^{+}$	20.69 (3)	3.60 (4)
$Gd + L \leftrightarrows GdL$	18.5 (2)	pGd: 19.3 (2)
$GdL + H \leftrightarrows GdLH$	23.5 (2)	5.0 (2)
$GdLH + H \leftrightarrows GdLH_2$	27.0 (5)	3.5 (5)
$Zn + L \leftrightarrows ZnL$	14.4 (2)	pZn: 15.2 (2)
$Ca + L \leftrightarrows CaL$	8.0 (3)	pCa: 8.8 (3)

Table 2. Association constants for the formation of the ternary complexes of oxalate and a bidentate 3,2-HOPO ligand with Ln-TREN-1,2-HOPO (Ln = Gd, Eu).

	Oxalate Relaxometry[a]	Oxalate Luminescence	3,2-HOPO Relaxometry[a]
$\log K_A$ (M^{-1})	1.90 (5)	2.0	3.5
r_{1p}^{bound} (mM^{-1} s^{-1})	5.5	-	5.2
r_{1p}^{free} (mM^{-1} s^{-1})	9.3	-	9.3

[a)] 20 MHz; 25 C

a) SYNOPSIS TOC.

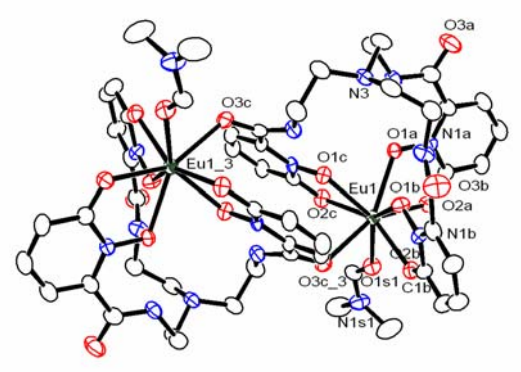

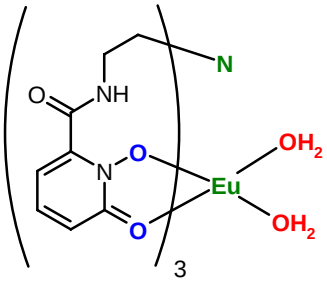

Luminescence

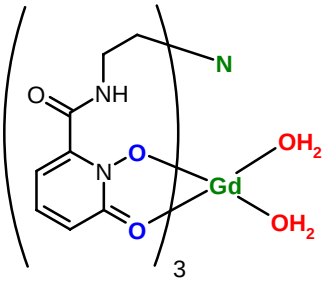

MRI

Gd-TREN-1,2-HOPO was investigated as a low toxicity and high relaxivity contrast agent for magnetic resonance imaging (MRI). Solution thermodynamics address the potential toxicity of Gd-TREN-1,2-HOPO. TREN-1,2-HOPO is selective for Gd(III) [pGd 19.3 (2)] versus Zn(II) [pZn 15.2 (2)] and Ca(II) [pCa 8.8 (3)]. Detailed solution thermodynamic studies applied fluorescence spectroscopy, potentiometric, spectrophotometric, NMR and relaxometric titrations. Photophysical measurements of the parent luminescent Eu(III) complex reveal insights into the solution structure of this family of lanthanide chelates.

References

[1] High Relaxivity Gadolinium MRI Agents. 22. Part 21: Jocher, C.J.; Botta, M.; Avedano, S.; Moore, E.G.; Xu, J.; Raymond, K.N., Inorg. Chem. 2007, ASAP.

[2] Cacheris, W. P.; Quay, S. C.; Rocklage, S. M. *Magn. Res. Imaging* **1990**, *8*, 467 – 481.

[3] Marckmann, P.; Skov, L.; Rossen, K.; Dupont, A.; Damholt, M. B.; Heaf, J. G.; Thomsen, H. S. *J. Am. Soc. Nephrol.* **2006**, *17*, 2359 – 2362.

[4] Caravan, P.; Ellison, J. J.; Murray, T. J.; Lauffer, R. B. *Chem. Rev*. **1999**, *99*, 2293 – 2352.

[5] Xu, J.; Franklin, S. J.; Whisenhunt Jr., D. W.; Raymond, K. N. *J. Am. Chem. Soc*. **1995**, *117*, 7245 – 7246.

[6] Werner, E. J., Avedano, S.; Botta, M.; Hay, B. P.; Moore, E. G., Aime, S.; Raymond, K. N. *J. Am. Chem. Soc*. **2007**, *129*, 1870 – 1871.

[7] Raymond, K. N.; Pierre, V. C. *Bioconjugate Chem*. **2005**, *16*, 3 – 8.

[8] Allen, M. J.; Raines, R. T.; Kiessling, L. L. *J. Am. Chem. Soc.* **2006**, *128*, 6534 – 6535.

[9] Pierre, V. C.; Botta, M.; Raymond, K. N. *J. Am. Chem. Soc*. **2005**, *127*, 504 – 505.

[10] Pierre, V. C.; Botta, M.; Aime, S.; Raymond, K. N. *J. Am. Chem. Soc.* **2006**, *128*, 9272 – 9273.

[11] Thompson, M. K.; Misselwitz, B.; Tso, L. S.; Doble,D. M. J.; Schmitt-Willich, H.; Raymond, K. N. *J. Med. Chem.* **2005**, *48*, 3874–3877.

[12] Peters, J. A.; Huskens, J.; Raber, D. J. *Progr. Nucl. Magn. Reson. Spectrosc*. **1996**, *28*, 283 – 350.

[13] De Horrocks, W. W. Jr.; Sudnick, D. R. *J. Am. Chem.. Soc.* **1979**, *101*, 334 – 340.

[14] Moore, E. G.; Xu, J.; Jocher, C. J.; Werner, E. J.; Raymond, K. N. *J. Am. Chem. Soc.* **2006**, *128*, 10067 – 10068.

[15] Xu, J.; Churchill, D. G.; Botta, M.; Raymond, K. N. *Inorg. Chem*. **2004**, *43*, 5492 – 5494.

[16] Johnson, A. R.; O´Sullivan, B.; Raymond, K. N. *Inorg. Chem*. **2000**, *39*, 2652 – 2660.

[17] Gans, P.; Sabatini, A.; Vacca, A. *Talanta* **1996**, *43*, 1739.

[18] Gans, P.; Sabatini, A.; Vacca, A. *Ann. Chim. (Rome)* **1999**, *89*, 45 – 49.

[19] Perin, D. D.; Dempsey, B. *Buffers for pH and Metal Ions Control*. Chapman and Hall: London, **1974**.

[20] Gottlieb, H.; Kotlyar, V.; Nudelman, A. *J. Org. Chem.* **1997**, *62*, 7512 – 7515.

[21] Doble, D. M. J.; Melchior, M.; O´Sullivan, B.; Siering, C.; Xu, J.; Pierre, V. C.; Raymond, K. N. *Inorg. Chem.* **2003**, *42*, 4930 – 4937.

[22] Xu, J.; Radkov, E.; Ziegler, M.; Raymond, K. N. *Inorg. Chem*. **2000**, *39*, 4156 – 4164.

[23] Kepert, D. L. *Prog. Inorg. Chem*. **1978**, *24*, 179.

[24] Beeby, A.; Clarckson, I. M.; Dickins, R. S.; Faulkner, S.; Parker, D.; Royle, L.; de Sousa, A. S.; Williams, J. A. G.; Woods, M. *J. Chem. Soc., Perkin Trans. 2* **1999**, 493 – 503.

[25] Bünzli, J. C. G.; Choppin, G. R.; Editors, *Lanthanide Probes in Life, Chemical and Earth Sciences: Theory and Practice.* **1989**.

[26] a) Murray, G. M., Sarrio, R. V., Peterson, J. R., *Inorg. Chim. Acta* **1990**, *176*, 233-240; b) Brecher, C., Samelson, H., Lempicki, A, *J. Chem. Phys*., **1965**, *42*, 1081-1096.

[27] Xu, J.; Whisenhunt Jr.; D. W.; Veeck, A. C.; Uhlir, L. C.; Raymond, K. N. *Inorg. Chem*. **2003**, *42*, 2665 – 2674.

[28] Cohen, S. M.; Meyer, M.; Raymond, K. N. *J. Am. Chem. Soc.* **1998**, *120*, 6277–6286.

[29] Cohen, S. M.; Raymond, K. N. *Inorg, Chem*. **2000**, *39*, 3624 – 3631.

[30] Baes, C. F. Jr.; Mesmer, R. E. *The Hydrolysis of Cations*, Krieger Publishing **1976**.

[31] Boyd, A. S.; Zic, J. A.; Abraham, J. L. *J. Am. Acad. Dermatol.* **2007**, *56*, 27 – 30.

[32] Li, Y. J.; Martell, A. E. *Inorg. Chim Acta* **1993**, *214*, 103 – 111.

[33] Pierre, V. C.; Botta, M.; Aime, S.; Raymond, K. N. *Inorg. Chem*. **2006**, *45*, 8355 – 8364.

[34] Dickins, R. S.; Aime, S.; Batsanov, A. S.; Beeby, A.; Botta, M.; Bruce, J. I.; Howard, J. A. K.; Love, C. S.; Parker, D.; Peacock, R. D.; Puschmann, H. *J. Am. Chem. Soc*. **2003**, *124*, 12697–12705.

[35] Botta, M.; Aime, S.; Barge, A.; Bobba, G.; Dickins, R. S.; Parker, D.; Terreno, E. *Chem. Eur. J.* **2003**, *9*, 2102–2109.

[36] Seitz, M.; Pluth, M. D.; Raymond, K. N. *Inorg. Chem.* **2007**, *46*, 351 – 353.